PHYSICAL REVIEW A **91**, 052323 (2015)

# Perfect wave-packet splitting and reconstruction in a one-dimensional lattice

Leonardo Banchi,* Enrico Compagno, and Sougato Bose
*Department of Physics and Astronomy, University College London, Gower Street, WC1E 6BT London, United Kingdom*
(Received 17 February 2015; published 22 May 2015)

Particle delocalization is a common feature of quantum random walks in arbitrary lattices. However, in the typical scenario a particle spreads over multiple sites and its evolution is not directly useful for controlled quantum interferometry, as may be required for technological applications. In this paper we devise a strategy to perfectly split the wave packet of an incoming particle into two components, each propagating in opposite directions, which reconstruct the shape of the initial wavefunction after a particular time $t^*$. Therefore, a particle in a $\delta$-like initial state becomes exactly delocalized between two distant sites after $t^*$. We find the mathematical conditions to achieve the perfect splitting, which are satisfied by viable example Hamiltonians with static site-dependent interaction strengths. Our results pave the way for the generation of peculiar many-body interference patterns in a many-site atomic chain (such as the Hanbury Brown and Twiss and quantum Talbot effects) as well as for the distribution of entanglement between remote sites. Thus, as for the case of perfect state transfer, the perfect wave-packet splitting can be a new tool for varied applications.

DOI: 10.1103/PhysRevA.91.052323 PACS number(s): 03.67.Hk, 05.60.Gg, 67.85.−d, 03.67.Bg

## I. INTRODUCTION

The quest for a quantum computer is boosting the development and engineering of new sophisticated quantum devices that allow us to observe the space-time evolution of its constituents. Indeed, in recent years several experimental groups successfully measured the quantum dynamical evolution of particles and/or quasiparticle hopping in a lattice [1–9]. Due to the inherent nature of quantum mechanics, the evolution of an isolated quantum system is represented by a wavefunction $\psi(x,t)$, which describes the probability amplitude of finding a particle in position $x$ at time $t$. Quantum interference can give rise to particular structures and patterns in the space-time evolution $|\psi(x,t)|^2$, which are known as "quantum carpets" [10], quantum revivals [11], or quantum Talbot effect [12,13], quantum walks [14–16], and quantum self-imaging [17].

An interesting case is when the wavefunction undergoes a revival, namely when after a particular time the shape of the initial wave packet is almost perfectly reconstructed. Aside from its fundamental implication, revivals occurring into a different position, far from the initial one, are particularly important for connecting and linking distant quantum registers [18,19]. On the other hand, a lattice of static localized particles represents an alternative paradigm for quantum communication where information carriers are not physically moving particles but rather collective excitations whose space extent is reconstructed at a different position after a certain time. In this respect, spin chains represent one of the most viable solutions and there are various protocols to exploit their dynamics for transferring states and entanglement between remote sites [20,21]. The coherent excitation transfer, or in general the wavefunction reconstruction at a certain time, corresponds to the phase alignment of the eigenstates entering into the wave packet and, as such, can happen only when the energy eigenvalues satisfy certain conditions [22,23]. Some models admitting a perfect [22,24,25] or almost perfect [26–29] reconstruction have been explicitly constructed. On the other hand, if the phase alignment is only between particular subsets of the energy eigenstates, then the wavefunction is split into a superposition of copies of the initial wave packet, each separated by a certain distance. This effect is known as fractional revival [11,22,30], or fractional Talbot effect [12].

In this paper we engineer a chain with nearest-neighbor interactions to obtain a perfect wave-packet splitting and reconstruction during a ballistic evolution. In other terms, if $\psi(x,t=0)=f(x)$ is the shape of the initial wave packet, at the revival time $t^*$ the wavefunction is $\psi(x,t)=\frac{f(x-vt^*)+f(x+vt^*)}{\sqrt{2}}$, where $v$ is the group velocity defined by the energy eigenvalues. While in general the revival time is connected to specific algebraic properties of the spectrum and might be very long, in our case the splitting happens on a time that is dictated by the group velocity of excitations and, as such, scales linearly with the distance. Our method is therefore specifically targeted for applications where a smaller operational time is particularly important for neglecting the interaction with the surrounding environment. Recently, it has been shown that the wavefunction of a one-dimensional excitation can be split into a transmitted and reflected components by introducing localized impurities [31–33] or via suitably designed time-dependent control fields [34]. Here we focus on a different strategy aiming at obtaining a *perfect* fractional revival.

The generalization of the fractional revival to a many-particle setting has many important applications. As far as identical particles (bosons/fermions) are concerned, it allows one to define a perfect effective beam-splitter operation between distant sites and then to observe multiparticle Hanbury Brown and Twiss interference effects [35,36], such as perfect bunching or antibunching. As for spin systems, that the perfect fractional revival can be used to generate dynamically long-distance entanglement, a topical application that may be tested experimentally with current technology [37,38]. Indeed, the use of particle delocalization to generate entanglement is particularly evident in a single excitation setup, namely when there is a single spin in the state $|\uparrow\rangle$ while all the other spins are in the state $|\downarrow\rangle$. If the wave packet of this excitation is perfectly

*Corresponding author: banchi.leonardo@gmail.com

 

split and reconstructed in two distant sites $n$ and $m$, then the final state of the spins pair $(n,m)$ is $(|\uparrow\downarrow\rangle_{nm} + |\downarrow\uparrow\rangle_{nm})/\sqrt{2}$, namely a maximally entangled Bell state. We show that this reasoning can also be used in a multiple excitation scenario to dynamically generate a maximal set of Bell pairs in a spin-chain setup, and to provide a more general version of previous proposals [39,40].

This paper is organized as follows. In Sec. II, we define the mathematical conditions that allow a particular fractional revival, namely the perfect splitting and reconstruction of an incoming wave packet, and we propose a numerical algorithm to find suitable Hamiltonians that will fulfill these conditions. Interesting applications are then analyzed in Sec. III in a many-particle setting. In particular, we discuss bunching and antibunching effects in atoms trapped in an optical lattice and the dynamical generation of entanglement in spin chains interacting with nearest-neighbor $XY$ couplings. Conclusions are drawn in Sec. IV.

## II. PERFECT SPLITTING WITH ENGINEERED COUPLINGS

We study a one-dimensional quantum walk in a lattice with nearest-neighbor engineered interactions described by the Hamiltonian

$$H_p = -\left(\sum_{n=1}^{L-1} J_n |n\rangle\langle n+1| + \text{H.c.}\right) - \sum_{n=1}^{L} B_n |n\rangle\langle n|, \quad (1)$$

where $|n\rangle$ represents the state where a particle is in the $n$th site, and $L$ is the length of the chain. To find the mathematical conditions for a perfect splitting and reconstruction, we first focus on the requirements to achieve perfect state transfer. To perfectly transfer an excitation from site 1 to site $L$, the coefficients $J_n$ and $B_n$ have to satisfy some conditions (see, e.g., Ref. [23]). First, the Hamiltonian has to be *mirror symmetric*; i.e., $J_{L-n}=J_n$ and $B_{L+1-n}=B_n$ for any $1 \leqslant n \leqslant L$. The mirror symmetry imposes some relations between the eigenvectors of the Hamiltonian [25]: if the eigenvalues $E_k$ of $H_p$ are ordered such that $E_k<E_{k+1}$, then

$$O_{Lk} = (-1)^k O_{1k}, \quad (2)$$

where $H_p = O E O^T$ is the eigenvalue decomposition of $H_p$. The second requirement is that the energy eigenvalues $E_k$ satisfy the relation

$$e^{-iE_k t^*} = (-1)^k e^{i\alpha}, \quad (3)$$

where $t^*$ is the transmission time and $\alpha$ is an arbitrary phase. Here we consider $\alpha = 0$, namely $\text{Tr}H = 0$. Among the analytic solutions of Eq. (3), the simplest one is given by the coupling pattern [24,41],

$$J_n^{\text{PST}} = \frac{\pi J}{2L}\sqrt{n(L-n)}, \quad B_n = 0, \quad (4)$$

which implements perfect state transfer (PST) at $t^* = L/J$. Other solutions can be obtained numerically using inverse eigenvalue algorithms [23,42,43]. If the eigenvalues and eigenvectors of $H_p$ satisfy Eqs. (2) and (3), then

$$\langle n|e^{-iH_p t^*}|m\rangle = \sum_k O_{n,k} O_{m,k} e^{-iE_k t^*} = \sum_k O_{n,k} O_{m,k} (-1)^k = \sum_k O_{n,k} O_{L+1-m,k} = \delta_{n,L+1-m}, \quad (5)$$

namely not only the dynamics implements a perfect transfer from site 1 to site $L$, but, more generally, an excitation initially located in site $m$ is perfectly transferred to site $L-m+1$ after a time $t^*$.

In a similar fashion, a perfect wave-packet splitting and reconstruction can be obtained when the eigenvalues of $H_p$ satisfy

$$e^{-iE_k t^*} = \cos\theta + i(-1)^k \sin\theta, \quad (6)$$

for some angle $\theta$. Indeed, by repeating Eq. (5) one finds $\langle n|e^{-iH_p t^*}|m\rangle = \cos\theta\ \delta_{nm} + i \sin\theta\ \delta_{n,L+1-m}$, namely

$$|m\rangle \xrightarrow{t^*} \cos\theta |m\rangle + i \sin\theta |L-m+1\rangle. \quad (7)$$

The eigenvalue relation, Eq. (6), is one of the main results of this paper. By properly choosing $\theta$ it is possible to balance the reconstruction on distant sites, as show in Eq. (7), and for $\theta = \pi/4$ one obtains the perfect delocalization between distant sites of an initially localized wave packet. The coupling pattern to satisfy Eq. (6) can be obtained using inverse eigenvalue techniques. From the conceptual point of view an inverse eigenvalue problem deals with finding the zeros of the highly nonlinear function $f(\lambda) = E(\lambda) - \tilde{E}$, where the vector $E(\lambda)$ contains the ordered eigenvalues of the Hamiltonian $H_p(\lambda)$ with parameters $\lambda$, and the vector $\tilde{E}$ contains the target spectrum. Among the algorithms to find the optimal parameters [44,45], the most used one relies on the application of the Newton method to find the zeros of $f(\lambda)$. The Newton method starts with an initial guess $\lambda^{(0)}$ and updates it according to the rule [46]

$$\mathcal{J}(\lambda_n)[\lambda^{(n+1)} - \lambda^{(n)}] = f(\lambda^{(n)}), \quad (8)$$

where the matrix, with elements

$$\mathcal{J}_{mk}(\lambda^{(n)}) = \frac{\partial f_m(\lambda^{(n)})}{\partial \lambda_k^{(n)}} = \langle m|O(\lambda^{(n)})^T \frac{\partial H_p(\lambda^{(n)})}{\partial \lambda_k^{(n)}} O(\lambda^{(n)})|k\rangle, \quad (9)$$

is the Jacobian matrix and $H_p(\lambda) = O(\lambda)E(\lambda)O(\lambda)^T$ is the eigenvalue decomposition of $H_p(\lambda)$. The linear system Eq. (8) has a unique solution provided that $\mathcal{J}$ is an invertible matrix. This in turn implies that the number of parameters have to match the number of eigenvalues, i.e., the dimension of the matrix.

The mirror symmetric Hamiltonian Eq. (1) has $L$ independent parameters, $L$ being the number of sites. Indeed, because of the mirror symmetry, when $L = 2N$ ($N$ being an integer) there are $N$ independent values of $J_n$ and $N$ independent values of $B_n$. On the other hand, when $L = 2N+1$, there are $N$ independent values of $J_n$ and $N+1$ independent values of $B_n$. We apply inverse eigenvalue techniques to find the coupling pattern, which allows a perfect balanced splitting of the wave packet. The latter is obtained by imposing the condition Eq. (6)

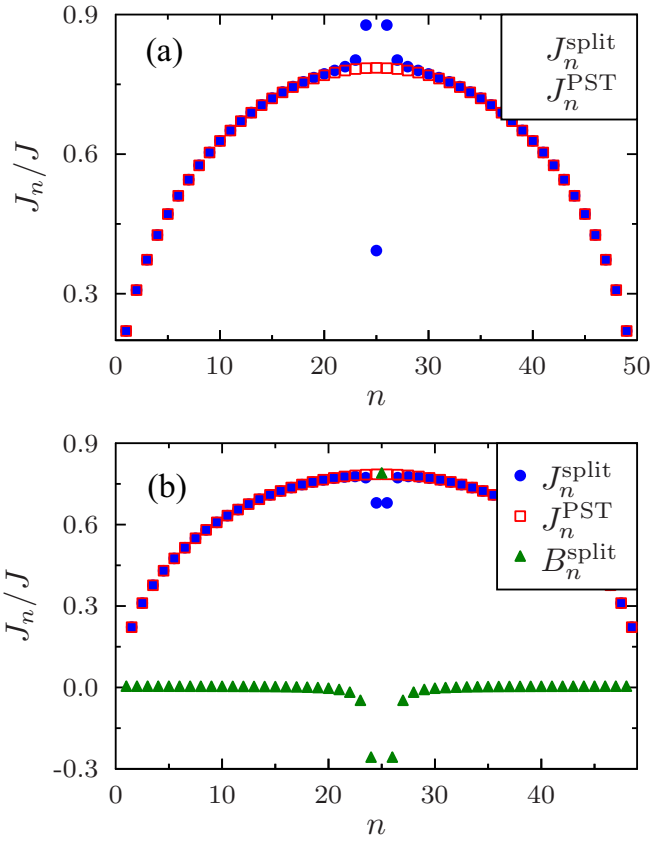


FIG. 1. (Color online) Comparison between the perfect wave-packet splitting couplings $J_n^{\rm split}$ and the perfect state transfer couplings $J_n^{\rm PST}$ in Eq. (4) for an even chain (a) and for an odd chain (b). Only in the latter case the perfect splitting requires also the engineering of a field profile $B_n^{\rm split}$.

with $\theta = \pi/4$, so the target eigenvalues are

$$\frac{L\tilde{E}}{J} = \left(\ldots, -\frac{\pi}{4}, \frac{\pi}{4}, -\frac{\pi}{4}+2\pi, \frac{\pi}{4}+2\pi, -\frac{\pi}{4}+4\pi, \ldots\right)^T, \tag{10}$$

where, without loss of generality, we have imposed $t^* = L/J$. Because $f(\lambda)$ is in general a nonconvex function, possibly with many local minima, inverse eigenvalue problems are known to converge only if the initial guess $\lambda^{(0)}$ is not too far from the ideal set of parameters $\tilde{\lambda}$ for which $E(\tilde{\lambda}) = \tilde{E}$ [46]. We guess that the optimal parameters for a perfect wave-packet splitting are given by a local perturbation of the fully engineered chain, which guarantees perfect state transfer, so we use the coupling pattern Eq. (4) as an initial condition.

The algorithm quickly converges to an optimal parameter set and hereinafter we called $J_n^{\rm split}$ and $B_n^{\rm split}$ the obtained optimal couplings and local fields. Surprisingly, we find that for even $L$ the algorithm always converges to a solution where $B_n^{\rm split} = 0$, while for odd $L$ the local fields $B_n^{\rm split}$ are different from zeros, especially near the center of the chain. For example, the Hamiltonians for $L = 5,6$ are shown in the Appendix. The output of the algorithm is shown in Fig. 1(a) for $L = 50$, and in Fig. 1(b) for $L = 49$. As it is clear, both for $L$ even and odd, the coupling patterns $J_n^{\rm split}$ for perfect wave-packet splitting are similar to the coupling pattern $J_n^{\rm PST}$, in Eq. (4), for perfect state transfer: the only difference being at the center of the chain. Moreover, for odd $L$ one requires also the engineering of the local fields $B_n^{\rm split}$ according to some particular profiles. The resulting field pattern is constant far from the center of the chain and has a particular oscillatory profile near the central sites.

## III. APPLICATIONS

### A. Perfect bunching and antibunching in a bosonic lattice

As a concrete application of the results of the last section we consider a model of hopping particle in a one-dimensional lattice, described by a Bose-Hubbard Hamiltonian with site-dependent parameters

$$\mathcal{H} = -\sum_{n=1}^{L} J_n(a_n^\dagger a_{n+1} + \text{H.c.}) + \sum_{n=1}^{L} U_n n_n(n_n - 1) - \sum_{n=1}^{L} B_n n_n. \tag{11}$$

Here $J_n = J_n^{\rm split}$ are the tunneling matrix elements, $U_n$ is the onsite interaction, $B_n = B_n^{\rm split}$ is the chemical potential, $a_n$ is the boson annihilation operator, and $n_j = a_j^\dagger a_j$. The Hamiltonian Eq. (11) accurately describes cold bosonic atoms in optical lattices [47,48], and it also models hard-core bosons [49] when $U \to \infty$ and, subsequently, under a Jordan-Wigner transformation, fermions [50,51]. Alternative implementations are systems of interacting polaritons [52] and coupled quantum dots [53]. Photonic lattices represent another promising system where $U_n = 0$ and the coupling strengths can be finely tuned [54]. In the optical lattice implementation the tuning of the site-dependent coupling constants in Eq. (11) is achieved via addressable optical lattices [55], created projecting an electric field profile via holographic masks [56,57] or via micromirror devices [1]. Initialization and read-out of single atoms are achieved exploiting single-particle addressing techniques [1,6,58–60] while magnetically induced Feshbach resonances allow a global control of the onsite interaction acting on the collisional coupling constants values [61]. For instance, the noninteracting regime $U_n = 0$ has been recently achieved with this technique using Cs atoms loaded in a one-dimensional optical lattice [62].

Thanks to the techniques developed in this paper, the coupling profile produces a splitting of a single-particle wavefunction, which is reconstructed at the transfer time $t^*$ as two copies of the initial wave packet with probability $1/2$ each. More precisely, when the coupling pattern $J_n^{\rm split}$ is implemented, the wavefunction of a bosonic atom initially onsite $n$ is split by the impurity pattern at the center of the lattice and, at the transfer time $t^*$, that particle is perfectly delocalized between two mirror symmetric sites, $n$ and $L - n + 1$. If an another particle was in the lattice in position $m$, after $t^*$ it would be delocalized between the sites $m$ and $L - m + 1$. When two particles are initially in two mirror symmetric sites, i.e., $m = L - n + 1$, the dynamics generates multiparticle Hanbury Brown and Twiss correlations [35] at $t^*$. Indeed, in the free-boson case, namely when $U_n = 0$, because

of the symmetries of the bosonic wavefunction, after a time $t^*$ the state becomes

$$|\psi(t^*)\rangle = \frac{|2\rangle_n|0\rangle_m + |0\rangle_n|2\rangle_m}{\sqrt{2}} \equiv |\psi_b\rangle, \tag{12}$$

i.e., the output state consists of a superposition of two bosons being in site $n$ and two bosons being in site $m = L - n + 1$. This "bunching" effect is the celebrated Hong-Ou-Mandel effect (HOM) [63], which has been observed recently exploiting the coherent evolution of two particles in a single double-well tunneling model [64]. With the results presented in this paper, because of the perfect reconstruction of wave packets at the transfer time, it is possible to achieve a perfect bunching between arbitrary distant sites of an optical lattice. On the other hand, one obtains antibunching in the hard-core boson limit $U_n = \infty$, where the final state is $|\psi(t^*)\rangle = |1\rangle_m|1\rangle_n$, i.e., there is one particle in position $n$ and one particle in position $m$.

#### 1. *Effect of imperfections in tuning the parameters*

In real systems, random noise effect, due to environmental variables, and engineering imperfections in the coupling configurations produce deviations from the ideal coupling values [55]. The effect of the coupling randomness, even for noninteracting systems, is to produce a localization of the eigenstates of the system and consequently to inhibit the state transfer [65]. We also mention that recently it has been shown [66,67] that the interaction of bosonic atoms with static fermionic impurities, randomly distributed in the lattice, may yield a Bose-Hubbard model where the parameters $J_n$ and $B_n$ are subject to noise. Given the above, we investigate what degree of imperfections is tolerable in our scheme or, in other terms, what is the precision required in tuning the coupling strengths according to the desired pattern.

We first include an off-diagonal disorder term (hopping disorder) in the Hamiltonian Eq. (11) as $J_n = J(J_n^{\text{split}} + x_n)$, where $x_n \in [-\epsilon, \epsilon]$ is a uniform random distribution and $\epsilon$ is the perturbation strength [68]. In Fig. 2(a) the relative variation $|\Delta P_{11}|/P_{11}(\epsilon = 0)$ is shown as a function of the degree of disorder $\epsilon$. Here $P_{11} = |\langle\psi_b|\psi(t^*)\rangle|^2$, where $|\psi_b\rangle$ is defined in Eq. (12), and $\Delta P \equiv |P_{11}(\epsilon) - P_{11}(\epsilon = 0)|$ represents the deviation of the bunching probability with respect to the ideal case. We also consider the effect of diagonal noise $B_j = B + Jx_j$ with $x_n \in [-\eta, \eta]$ in an even site chain. The effect of signal noise is shown in Fig. 2(b) as a function of the noise coupling strength $\epsilon$. As is clear from Figs. 2(a) and 2(b), a power-law behavior, under a certain threshold value of $\epsilon$ and $\eta$, characterizes both the deviations due to hopping disorder and due to the diagonal disorder. Clearly, an high degree of disorder produces state localization, which completely destroys the effect.

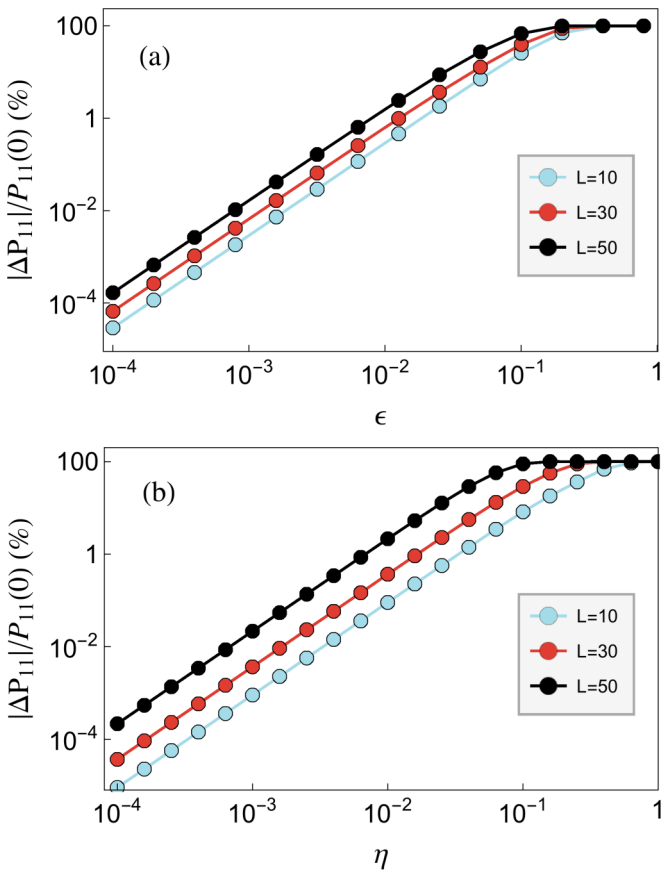


FIG. 2. (Color online) Relative variation of the bunching probability $P_{11}(t = t^*)$ in the noninteracting regime $U_n = 0$, in the presence of (a) random hopping noise and (b) random diagonal noise, respectively, with coupling strength $\epsilon$ and $\eta$. Several chain lengths $L$ are considered.

### B. Quantum many-particle carpets

The perfect reconstruction scheme developed in the previous sections enables the generation of periodic space-time quantum interference patterns, known as "quantum carpets," which resemble the Talbot effect [12] and generalize it to a quantum many-particle lattice. By using the engineered chain

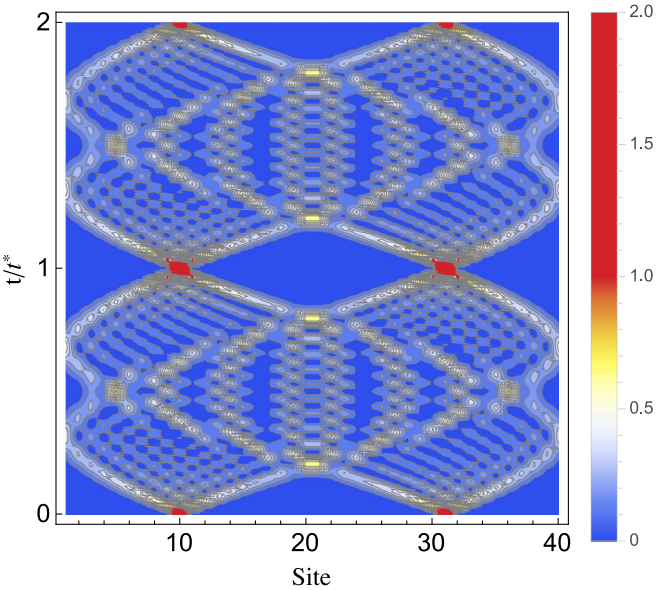


FIG. 3. (Color online) Quantum carpet: space-time evolution of $\langle n_j^2(t)\rangle$ for a $L = 40$ one-dimensional chain initialized in $|\psi_0\rangle = a_{10}^\dagger a_{31}^\dagger|0\rangle$. We consider the free-boson regime $U_n = 0$.

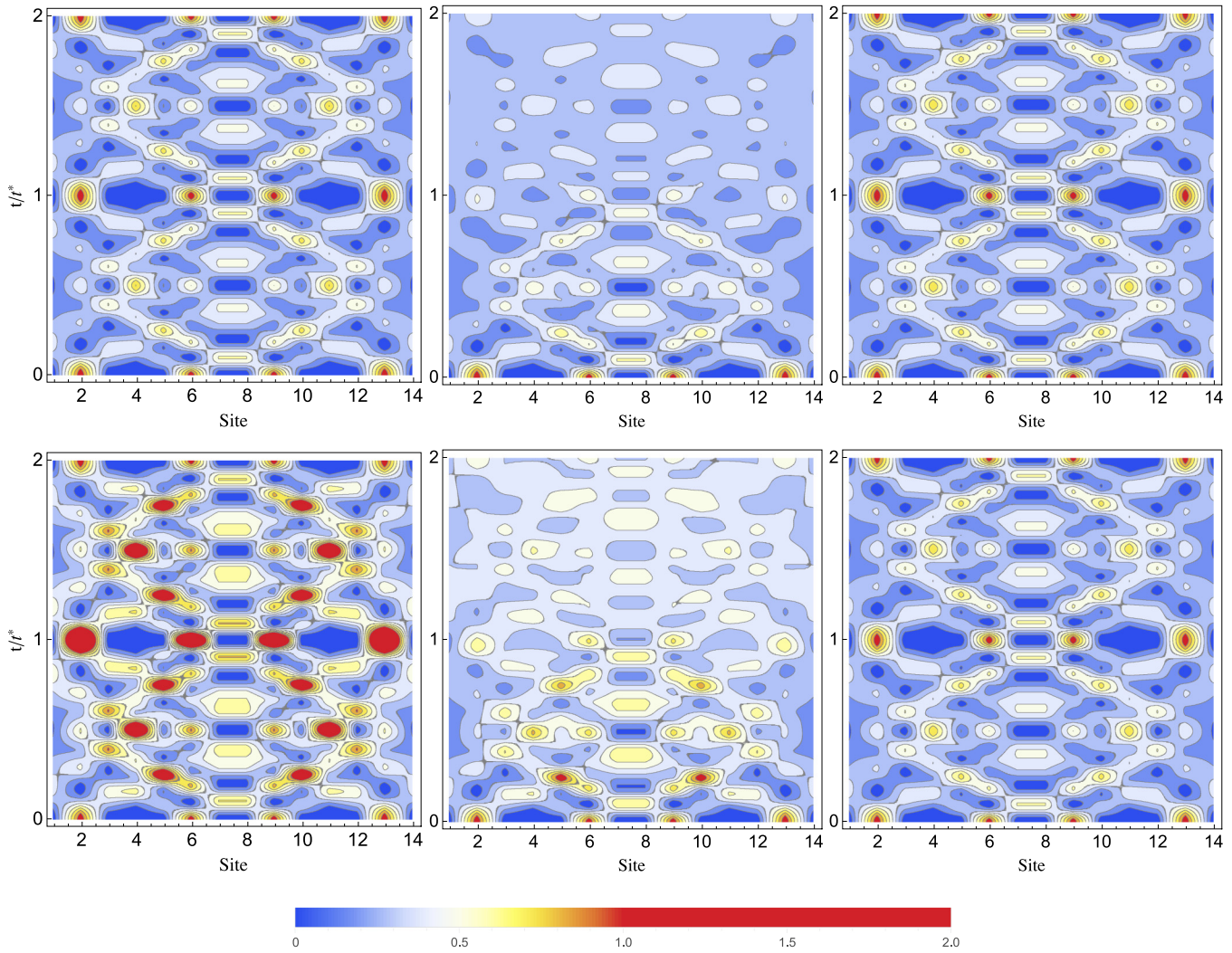


FIG. 4. (Color online) Quantum carpet due to four-particle interference. The initial state $|\psi_0\rangle = a_2^\dagger a_6^\dagger a_9^\dagger a_{13}^\dagger |0\rangle$ contains four bosonic particles. We consider the space-time evolution of $\langle n_j(t)\rangle$ in the top row and the space-time evolution of $\langle n_j^2(t)\rangle$ in the bottom row. The chain length is $L = 14$ and several values of the onsite interaction $U_n = U$ are considered: $U = 0$ (left column), $U = 1$ (center column), and $U = 30$ (right column). Here $t^*$ (expressed in J units) is the fractional revival time, while $2t^*$ is the full revival time. The difference between the first and second row is due to bunching and antibunching effects. Note the transition from bosonic ($U = 0$) to fermionic and hard-core boson ($U = \infty$) behavior as a function of $U$.

with $J_n^{\text{split}}$ and $B_n^{\text{split}}$, one in fact expects a regular temporal pattern in the evolution: the wave packets composing the initial state are split into two copies, reconstructed into different positions after the time $t^*$, and then they go back to the initial position after a time $2t^*$. On the other hand, during intermediate times, quantum interference leads to different behaviors, which are expected to be susceptible to the particle statistics. To show this effect, we study the quantum carpet generated by the space-time evolution of the mean occupation number $\langle n_j(t)\rangle$ or by the square occupation mean $\langle n_j^2(t)\rangle$. The regular interference pattern of a two-particle system is depicted in Fig. 3, where we show the expectation value $\langle n_j^2(t)\rangle$ for two noninteracting bosons initially in $|\psi_0\rangle = a_{10}^\dagger a_{31}^\dagger |0\rangle$ in a one-dimensional chain with $L = 40$.

To highlight more in detail the multiparticle statistical interference effect we consider a system of four particles, initially in $|\psi_0\rangle = a_2^\dagger a_6^\dagger a_9^\dagger a_{13}^\dagger |0\rangle$, where $L = 14$. We show in Figs. 4(a) and 4(d), respectively, the mean occupation number and the mean-square occupation number for the noninteracting case and for the strong-interacting case in Figs. 4(c) and 4(f). In the boson case bunching effects are observable at $t^*$, while in both cases a perfect reconstruction of the initial wave packet happens at $2t^*$. This is evident more clearly in Fig. 5, where we represent the mean occupation number and the mean-square occupation number of site 2 as a function of time. We also take into consideration the role of the onsite interaction, which affects the perfect reconstruction of a two-particle wave packet. It turns out that from the space-time dynamics of $\langle n_j(t)\rangle$ it is not possible to discriminate free evolution ($U = 0$) from the hard-core limit ($U = \infty$), while particle statistics give rise to different dynamics for $\langle n_j^2(t)\rangle$. On the other hand, for intermediate values of the onsite interaction the Hamiltonian cannot be mapped into a free model (either bosonic or fermionic), so scattering effects prevent the perfect reconstruction of the wave packet. This effect is clearly shown

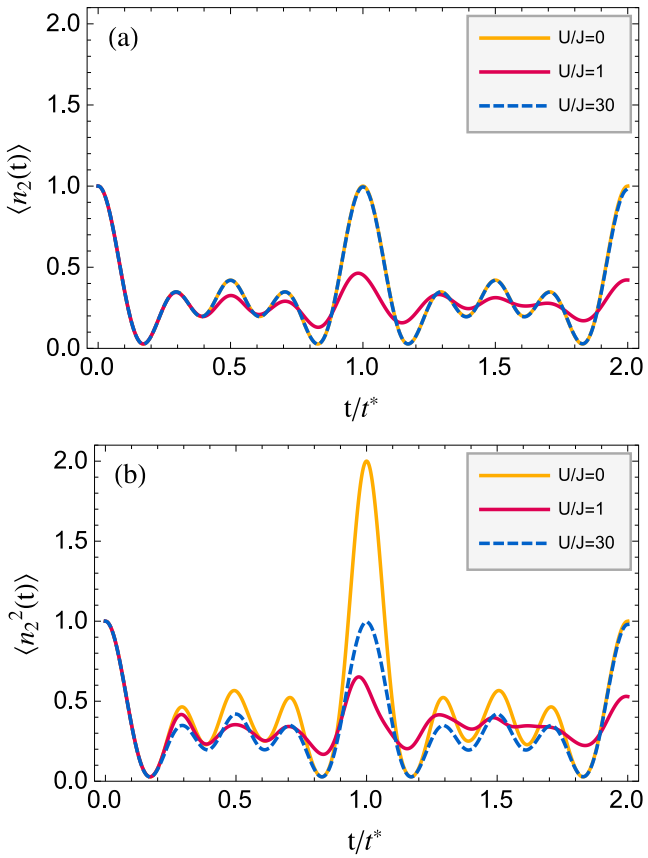


FIG. 5. (Color online) Plot of the (a) mean occupation number and of the (b) mean-square occupation number of site 2 as a function of time $t$ for several values of the onsite interaction. Here $L = 14$ and the initial state is $|\psi(0)\rangle = a_2^\dagger a_6^\dagger a_9^\dagger a_{13}^\dagger |0\rangle$. Note the transition from bosonic ($U = 0$) to fermionic and hard-core boson ($U = \infty$) behavior as a function of $U$.

in Figs. 4(b) and 4(e) and in Fig. 5 for $U_n = 1$, where $\langle n_2^2(t = 2t^*)\rangle < \langle n_2^2(t = 0)\rangle$ and $\langle n_2(t = 2t^*)\rangle < \langle n_2(t = 0)\rangle$.

From Fig. 4 one may also notice a partial fractional revival for $t = t^*/2$ and $t = t^*/4$. In Fig. 6 we show the results for $\langle n_j(t = t^*/4)\rangle$ and $\langle n_j^2(t = t^*/4)\rangle$.

### C. Perfect generation of entanglement in an $XY$ spin chain

We now consider a chain of spin-$\frac{1}{2}$ magnets described by the $XY$ Hamiltonian

$$\mathcal{H} = -\sum_n (J_n \sigma_n^+ \sigma_{n+1}^- + \text{H.c.}) - \sum_n \frac{B_n}{2}\sigma_n^z, \qquad (13)$$

where $\sigma_n^\alpha$, $\alpha = x, y, z$ are the Pauli spin operators acting on the spin localized in the $n$th site of the chain, and $\sigma_n^\pm = (\sigma_n^x \pm i\sigma_n^y)/2$. Effective spin-$\frac{1}{2}$ systems coupled by the Hamiltonian Eq. (13) with site-dependent coupling strengths can be obtained in different physical realizations; e.g., in NRM using global rotations and suitable field gradients [69], with atomic ions confined in segmented microtraps [70], with neutral atoms trapped into an optical lattice by polarized laser beams [3,71], or with superconducting qubits coupled either by site-dependent capacitors [72] or inductors [73].

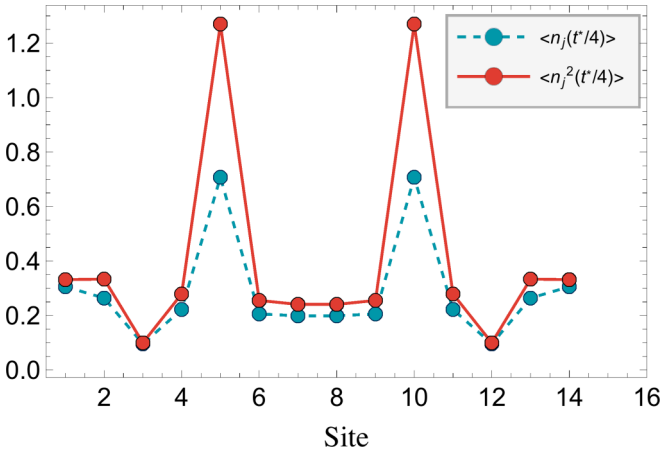


FIG. 6. (Color online) Plot of the mean occupation number and of the mean-square occupation number for each site at $t = t^*/4$ for $U/J = 0$. Here $L = 14$ and the initial state is $|\psi(0)\rangle = a_2^\dagger a_6^\dagger a_9^\dagger a_{13}^\dagger |0\rangle$.

The system Hamiltonian Eq. (13) can be mapped to a fermionic hopping model via the Jordan-Wigner transformation: the operators $c_n = \prod_{j<n}(-\sigma_j^z)\sigma_n^-$ satisfy canonical anticommutation relations and $\mathcal{H} = \sum_{nm}\langle n|H|m\rangle\, c_n^\dagger c_m$, where $H$ is the hopping matrix Eq. (1). Every many-body spin state can be obtained by applying the annihilation operators $c_n$ to the fully polarized state $|\Omega\rangle = |\uparrow\uparrow\cdots\rangle$. Therefore, the time evolution of a generic initial state can be obtained by expressing the operator $c_n$ in the Heisenberg picture [27] as

$$c_n(t) = \sum_m \langle n|e^{-iHt}|m\rangle\, c_m. \qquad (14)$$

We now show how one can create entanglement between two remote mirror symmetric sites by exploiting the perfect wave-packet splitting Eq. (7). Suppose that, starting from the fully polarized state $|\Omega\rangle$ a particle is flipped in position $n$; the initial state of the system is then $c_n|\Omega\rangle$. When the single-particle Hamiltonian implements the transformation Eq. (7), then, thanks to Eq. (14) one has $c_n|\Omega\rangle \xrightarrow{t^*} (c_n|\Omega\rangle + i c_{L-n+1}|\Omega\rangle)/\sqrt{2}$. Therefore, going back to the spin picture, after the time $t^*$ an entangled state $\frac{|\uparrow\downarrow\rangle + i|\downarrow\uparrow\rangle}{\sqrt{2}}$ between sites $n$ and $L - n + 1$ is generated.

The above arguments can be generalized in a many-particle setting to generate the maximal amount of entangled pairs starting from a separable state. Two suitable choices of the initial state are

$$|\psi^{\text{DM}}\rangle = |\uparrow\uparrow\cdots\uparrow\downarrow\cdots\downarrow\downarrow\rangle, \qquad (15)$$

$$|\psi^{\text{AFM}}\rangle = |\uparrow\downarrow\uparrow\cdots\uparrow\downarrow\rangle, \qquad (16)$$

namely the domain-wall state $|\psi^{\text{DM}}\rangle$ or the antiferromagnetic state $|\psi^{\text{AFM}}\rangle$. If the system is initialized in either $|\psi^{\text{DM}}\rangle$ or $|\psi^{\text{AFM}}\rangle$ and is let to evolve under the perfect splitting Hamiltonian, then the resulting state after a time $t^*$ is $(c_1 + e^{i\alpha_1}c_L)(c_2 + e^{i\alpha_2}c_{L-1})(c_3 + e^{i\alpha_3}c_{L-2})\cdots|\Omega\rangle$, where $\alpha_i$ depends on the initial state. By carefully dealing with the Jordan-Wigner phase entering into the definition of the operators $c_n$, one can easily find that the resulting state corresponds to a state in which every pair of qubits sitting

in positions $n$ and $L-n+1$ is maximally entangled, namely $|\psi_{n,L-n+1}(t^*)\rangle = (|\uparrow\downarrow\rangle + e^{i\alpha'_n}|\downarrow\uparrow\rangle)/2$, where $\alpha'_n$ can differ from $\alpha_n$ by a $\pi$ factor. The perfect splitting dynamics thus represents an alternative to other methods existing in the literature to generate nested Bell pairs [39,40] starting from a separable state. However, compared to previous proposals it is more general because it allows tuning the number of generated Bell pairs by simply choosing the number of flipped spins in the initial state.

## IV. CONCLUSIONS

In this paper we study the wavefunction dynamics of hopping particles and/or quasiparticles in a quantum chain. We design the Hamiltonian so that a localized wave packet evolves coherently along the chain without dispersion and at a particular point is perfectly split into transmitted and reflected components that propagate in opposite directions without dispersion. When the reflected component reaches the initial site, its wave packet becomes localized while, at the same time, the wave packet of the transmitted component becomes localized in a different site of the chain. We devise the exact conditions that the Hamiltonian spectrum has to satisfy to allow for the perfect splitting and reconstruction. Then we focus on some viable Hamiltonians with nearest-neighbor interactions and site-dependent couplings, and we find the coupling pattern that satisfies the perfect splitting condition using inverse eigenvalue techniques.

Besides shedding light into quantum interference phenomena in one dimension, our results are particularly useful for applications. In this respect, we study atomic lattices and obtain perfect Hanbury Brown and Twiss correlations and peculiar quantum interference patterns that result in regular structure in the space-time evolution of the many-particle wavefunction. Moreover, we show that in a spin-chain setting, the particle splitting can be used to generate maximally entangled states between distant parts.

We expect that the perfect wave-packet splitting will become a general tool for varied applications in controlled quantum interference and quantum information processing.

## ACKNOWLEDGMENT

The research leading to these results has received funding from the European Research Council under the European Union's Seventh Framework Programme (FP/2007-2013)/ ERC Grant Agreement No. 308253.

## APPENDIX: PERFECT SPLITTING HAMILTONIAN FOR $L = 5,6$

The Hamiltonian matrices $\langle n|H|m\rangle$ for perfect balanced splitting when $L = 5$ and 6 are, respectively (in unit of $J$):

$$\begin{pmatrix} -0.08378 & 0.6195 & 0 & 0 & 0 \\ 0.6195 & -0.2932 & 0.6664 & 0 & 0 \\ 0 & 0.6664 & 0.7540 & 0.6664 & 0 \\ 0 & 0 & 0.6664 & -0.2932 & 0.6195 \\ 0 & 0 & 0 & 0.6195 & -0.08378 \end{pmatrix}$$

$$\begin{pmatrix} 0 & 0.5999 & 0 & 0 & 0 & 0 \\ 0.5999 & 0 & 0.8279 & 0 & 0 & 0 \\ 0 & 0.8279 & 0 & 0.3927 & 0 & 0 \\ 0 & 0 & 0.3927 & 0 & 0.8279 & 0 \\ 0 & 0 & 0 & 0.8279 & 0 & 0.5999 \\ 0 & 0 & 0 & 0 & 0.5999 & 0 \end{pmatrix}.$$

As shown in Sec. III, small imperfections parameter tuning result in negligible deviations from the ideal dynamics.


[1] P. M. Preiss, R. Ma, M. E. Tai, A. Lukin, M. Rispoli, P. Zupancic, Y. Lahini, R. Islam, and M. Greiner, Science **347**, 1229 (2015).

[2] T. Fukuhara, A. Kantian, M. Endres, M. Cheneau, P. Schauß, S. Hild, D. Bellem, U. Schollwöck, T. Giamarchi, C. Gross, I. Bloch, and S. Kuhr, Nat. Phys. **9**, 235 (2013).

[3] T. Fukuhara, P. Schauß, M. Endres, S. Hild, M. Cheneau, I. Bloch, and C. Gross, Nature **502**, 76 (2013).

[4] L. Sansoni, F. Sciarrino, G. Vallone, P. Mataloni, A. Crespi, R. Ramponi, and R. Osellame, Phys. Rev. Lett. **108**, 010502 (2012).

[5] C. Ramanathan, P. Cappellaro, L. Viola, and D. G. Cory, New J. Phys. **13**, 103015 (2011).

[6] M. Schreiber, S. S. Hodgman, P. Bordia, H. P. Lüschen, M. H. Fischer, R. Vosk, E. Altman, U. Schneider, and I. Bloch, arXiv:1501.05661 (2015).

[7] P. Richerme, Z.-X. Gong, A. Lee, C. Senko, J. Smith, M. Foss-Feig, S. Michalakis, A. V. Gorshkov, and C. Monroe, Nature **511**, 198 (2014).

[8] J. Schachenmayer, B. P. Lanyon, C. F. Roos, and A. J. Daley, Phys. Rev. X **3**, 031015 (2013).

[9] H. Trompeter, T. Pertsch, F. Lederer, D. Michaelis, U. Streppel, A. Bräuer, and U. Peschel, Phys. Rev. Lett. **96**, 023901 (2006).

[10] A. E. Kaplan, I. Marzoli, W. E. Lamb, and W. P. Schleich, Phys. Rev. A **61**, 032101 (2000).

[11] R. W. Robinett, Phys. Rep. **392**, 1 (2004).

[12] M. Berry, I. Marzoli, and W. Schleich, Phys. World **14**, 39 (2001).

[13] X.-B. Song, H.-B. Wang, J. Xiong, K. Wang, X. Zhang, K.-H. Luo, and L.-A. Wu, Phys. Rev. Lett. **107**, 033902 (2011).

[14] J. Kempe, Contemp. Phys. **44**, 307 (2003).

[15] A. M. Childs, Phys. Rev. Lett. **102**, 180501 (2009).

[16] A. M. Childs, R. Cleve, E. Deotto, E. Farhi, S. Gutmann, and D. A. Spielman, in *Proceedings of the Thirty-fifth Annual ACM Symposium on Theory of Computing*, STOC '03 (ACM, New York, 2003), pp. 59–68.

[17] S. Longhi, Phys. Rev. B **82**, 041106 (2010).

[18] J. I. Cirac, P. Zoller, H. J. Kimble, and H. Mabuchi, Phys. Rev. Lett. **78**, 3221 (1997).

[19] S. Ritter, C. Nölleke, C. Hahn, A. Reiserer, A. Neuzner, M. Uphoff, M. Mücke, E. Figueroa, J. Bochmann, and G. Rempe, Nature **484**, 195 (2012).

[20] S. Bose, Contemp. Phys. **48**, 13 (2007).

[21] G. M. Nikolopoulos and I. Jex, eds., *Quantum State Transfer and Network Engineering*, 2014th ed. (Springer, New York, 2013).

[22] D. L. Aronstein and C. R. Stroud, Phys. Rev. A **55**, 4526 (1997).

[23] A. Kay, Int. J. Quantum Inf. **08**, 641 (2010).

[24] C. Albanese, M. Christandl, N. Datta, and A. Ekert, Phys. Rev. Lett. **93**, 230502 (2004).

[25] M.-H. Yung and S. Bose, Phys. Rev. A **71**, 032310 (2005).

[26] C. Godsil, S. Kirkland, S. Severini, and J. Smith, Phys. Rev. Lett. **109**, 050502 (2012).

[27] L. Banchi, Eur. Phys. J. Plus **128**, 1 (2013).

[28] L. Banchi, T. J. G. Apollaro, A. Cuccoli, R. Vaia, and P. Verrucchi, New J. Phys. **13**, 123006 (2011).

[29] N. Y. Yao, L. Jiang, A. V. Gorshkov, Z.-X. Gong, A. Zhai, L.-M. Duan, and M. D. Lukin, Phys. Rev. Lett. **106**, 040505 (2011).

[30] B. Chen, Z. Song, and C. P. Sun, Phys. Rev. A **75**, 012113 (2007).

[31] E. Compagno, L. Banchi, and S. Bose, arXiv:1407.8501 (2014).

[32] T. Fogarty, A. Kiely, S. Campbell, and T. Busch, Phys. Rev. A **87**, 043630 (2013).

[33] B. Gertjerenken, Phys. Rev. A **88**, 053623 (2013).

[34] M. I. Makin, J. H. Cole, C. D. Hill, and A. D. Greentree, Phys. Rev. Lett. **108**, 017207 (2012).

[35] R. H. Brown and R. Q. Twiss, Nature **177**, 27 (1956).

[36] Y. Lahini, M. Verbin, S. D. Huber, Y. Bromberg, R. Pugatch, and Y. Silberberg, Phys. Rev. A **86**, 011603 (2012).

[37] C. Mitra, Nat. Phys. **11**, 212 (2015).

[38] S. Sahling, G. Remenyi, C. Paulsen, P. Monceau, V. Saligrama, C. Marin, A. Revcolevschi, L. P. Regnault, S. Raymond, and J. E. Lorenzo, Nat. Phys. **11**, 255 (2015).

[39] B. Alkurtass, L. Banchi, and S. Bose, Phys. Rev. A **90**, 042304 (2014).

[40] C. Di Franco, M. Paternostro, and M. S. Kim, Phys. Rev. A **77**, 020303 (2008).

[41] M. Christandl, N. Datta, A. Ekert, and A. J. Landahl, Phys. Rev. Lett. **92**, 187902 (2004).

[42] A. Kay, Phys. Rev. A **73**, 032306 (2006).

[43] M. Bruderer, K. Franke, S. Ragg, W. Belzig, and D. Obreschkow, Phys. Rev. A **85**, 022312 (2012).

[44] B. Parlett, *The Symmetric Eigenvalue Problem*, Classics in Applied Mathematics (Society for Industrial and Applied Mathematics, Philadelphia, PA, 1998).

[45] M. Chu, SIAM Rev. **40**, 1 (1998).

[46] S. Friedland, J. Nocedal, and M. L. Overton, SIAM J. Numer. Anal. **24**, 634 (1987).

[47] D. Jaksch, C. Bruder, J. I. Cirac, C. W. Gardiner, and P. Zoller, Phys. Rev. Lett. **81**, 3108 (1998).

[48] M. Greiner, O. Mandel, T. Esslinger, T. W. Hänsch, and I. Bloch, Nature **415**, 39 (2002).

[49] M. Rigol and A. Muramatsu, Phys. Rev. A **70**, 031603 (2004).

[50] R. Jördens, N. Strohmaier, K. Günter, H. Moritz, and T. Esslinger, Nature **455**, 204 (2008).

[51] G. Modugno, F. Ferlaino, R. Heidemann, G. Roati, and M. Inguscio, Phys. Rev. A **68**, 011601 (2003).

[52] M. J. Hartmann, F. G. Brandao, and M. B. Plenio, Nat. Phys. **2**, 849 (2006).

[53] G. M. Nikolopoulos, D. Petrosyan, and P. Lambropoulos, J. Phys.: Condens. Matter **16**, 4991 (2004).

[54] M. Bellec, G. M. Nikolopoulos, and S. Tzortzakis, Opt. Lett. **37**, 4504 (2012).

[55] Z.-M. Wang, L.-A. Wu, M. Modugno, W. Yao, and B. Shao, Sci. Rep. **3**, 3128 (2013).

[56] W. S. Bakr, J. I. Gillen, A. Peng, S. Fölling, and M. Greiner, Nature **462**, 74 (2009).

[57] V. Boyer, R. M. Godun, G. Smirne, D. Cassettari, C. M. Chandrashekar, A. B. Deb, Z. J. Laczik, and C. J. Foot, Phys. Rev. A **73**, 031402 (2006).

[58] C. Weitenberg, M. Endres, J. F. Sherson, M. Cheneau, P. Schauß, T. Fukuhara, I. Bloch, and S. Kuhr, Nature **471**, 319 (2011).

[59] M. Endres, M. Cheneau, T. Fukuhara, C. Weitenberg, P. Schauß, C. Gross, L. Mazza, M. C. Bañuls, L. Pollet, I. Bloch, and S. Kuhr, Appl. Phys. B **113**, 27 (2013).

[60] C. Gross and I. Bloch, arXiv:1409.8501 (2014).

[61] J. C. Sanders, O. Odong, J. Javanainen, and M. Mackie, Phys. Rev. A **83**, 031607 (2011).

[62] F. Meinert, M. J. Mark, E. Kirilov, K. Lauber, P. Weinmann, M. Gröbner, and H.-C. Nägerl, Phys. Rev. Lett. **112**, 193003 (2014).

[63] C. K. Hong, Z. Y. Ou, and L. Mandel, Phys. Rev. Lett. **59**, 2044 (1987).

[64] A. M. Kaufman, B. J. Lester, C. M. Reynolds, M. L. Wall, M. Foss-Feig, K. R. A. Hazzard, A. M. Rey, and C. A. Regal, Science **345**, 306 (2014).

[65] J. P. Keating, N. Linden, J. C. F. Matthews, and A. Winter, Phys. Rev. A **76**, 012315 (2007).

[66] J. Stasińska, M. Łącki, O. Dutta, J. Zakrzewski, and M. Lewenstein, Phys. Rev. A **90**, 063634 (2014).

[67] S. Ospelkaus, C. Ospelkaus, O. Wille, M. Succo, P. Ernst, K. Sengstock, and K. Bongs, Phys. Rev. Lett. **96**, 180403 (2006).

[68] A. Zwick, G. A. Álvarez, J. Stolze, and O. Osenda, Phys. Rev. A **84**, 022311 (2011).

[69] A. Ajoy and P. Cappellaro, Phys. Rev. Lett. **110**, 220503 (2013).

[70] H. Wunderlich, C. Wunderlich, K. Singer, and F. Schmidt-Kaler, Phys. Rev. A **79**, 052324 (2009).

[71] L.-M. Duan, E. Demler, and M. D. Lukin, Phys. Rev. Lett. **91**, 090402 (2003).

[72] M. Neeley, R. C. Bialczak, M. Lenander, E. Lucero, M. Mariantoni, A. D. O'Connell, D. Sank, H. Wang, M. Weides, J. Wenner, Y. Yin, T. Yamamoto, A. N. Cleland, and J. M. Martinis, Nature **467**, 570 (2010).

[73] Y. Chen, C. Neill, P. Roushan, N. Leung, M. Fang, R. Barends, J. Kelly, B. Campbell, Z. Chen, B. Chiaro, A. Dunsworth, E. Jeffrey, A. Megrant, J. Y. Mutus, P. J. J. O'Malley, C. M. Quintana, D. Sank, A. Vainsencher, J. Wenner, T. C. White, M. R. Geller, A. N. Cleland, and J. M. Martinis, Phys. Rev. Lett. **113**, 220502 (2014).